

Coherent Vector Meson Production in Ultra-Peripheral Heavy-Ion Collisions at STAR

F. Meissner ^a, for the STAR Collaboration ^{*}

^aLawrence Berkeley National Laboratory
One Cyclotron Rd., Berkeley, CA 94720

We report the first observation of coherent ρ^0 production ($AuAu \rightarrow AuAu\rho^0$) and ρ^0 production accompanied by mutual nuclear Coulomb excitation ($AuAu \rightarrow Au^*Au^*\rho^0$), and the observation of coherent e^+e^- pair production ($AuAu \rightarrow Au^*Au^*e^+e^-$) in ultra-peripheral relativistic heavy-ion collisions (UPCs). We give transverse momentum, mass, and rapidity distributions. The cross sections for coherent ρ^0 production at $\sqrt{s_{NN}} = 130$ and 200 GeV are in agreement with theoretical predictions, which treat ρ^0 production and nuclear excitation as independent processes.

In ultra-peripheral heavy ion collisions, photon exchange, photon-photon or photon-nuclear interactions take place at impact parameters b larger than twice the nuclear radius R_A , where no nucleon-nucleon collisions occur [1]. Examples are nuclear Coulomb excitation, electron-positron pair and meson production, and vector meson production.

Exclusive ρ^0 meson production, $AuAu \rightarrow AuAu\rho^0$ (Fig. 1a), can be described by the Weizsäcker-Williams approach [2] to the photon flux and the vector meson dominance model [3]. A photon emitted by one nucleus fluctuates to a virtual ρ^0 meson, which scatters elastically from the other nucleus. The gold nuclei are not disrupted, and the final state consists solely of the two nuclei and the vector meson decay products [4]. In addition to coherent ρ^0 production, the exchange of virtual photons may excite the nuclei (Fig. 1b), yielding

the subsequent emission of single (1n) or multiple (xn) neutrons; these processes are assumed to factorize for heavy-ion collisions. In the rest frame of the target nucleus, mid-rapidity ρ^0 production at RHIC corresponds to a photon energy of 50 GeV and a photon-nucleon center-of-mass energy of 10 GeV. At this energy, Pomeron (\mathcal{P}) exchange dominates over meson exchange, as indicated by the rise of the ρ^0 production cross section with increasing energy in lepton-nucleon scattering.

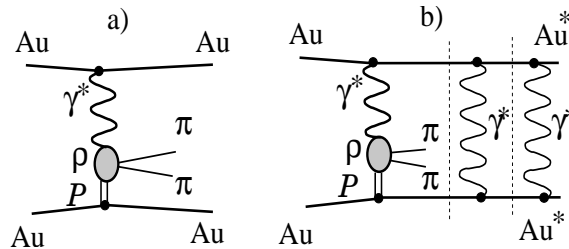


Figure 1: Diagram for (a) exclusive ρ^0 production in ultra-peripheral heavy ion collisions, and (b) ρ^0 production with nuclear excitation. The dashed lines indicate factorization.

^{*}For the full author list and acknowledgements, see Appendix "Collaborations" of this volume.

The photon and Pomeron can couple coherently to the nuclei. The wavelength $\lambda_{\gamma,P} > 2R_A$ leads to coherence conditions: a low transverse momentum of $p_T < \pi\hbar/R_A$ (~ 90 MeV/c for gold with $R_A \sim 7$ fm), and a maximum longitudinal momentum of $p_{\parallel} < \pi\hbar\gamma/R_A$ ($\sim 6(9)$ GeV/c at $\gamma=70(100)$), where γ is the Lorentz boost of the nucleus. The photon flux is proportional to the square of the nuclear charge Z^2 [2], and the forward cross section for elastic $\rho^0 A$ scattering $d\sigma^{\rho^0 A}/dt|_{t=0}$ scales as $A^{4/3}$ for surface coupling and A^2 in the bulk limit. The ρ^0 production cross sections are large. At a center-of-mass energy of $\sqrt{s_{NN}} = 130(200)$ GeV, a total ρ^0 cross section, regardless of nuclear excitation, $\sigma(AuAu \rightarrow Au^{(*)}Au^{(*)}\rho^0) = 350(590)$ mb is predicted from a Glauber extrapolation of $\gamma p \rightarrow \rho^0 p$ data [4]. Calculations for coherent ρ^0 production with nuclear excitation assume that both processes are independent, sharing only a common impact parameter [4, 5].

In the years 2000 and 2001, RHIC collided gold nuclei at a center-of-mass energy of $\sqrt{s_{NN}} = 130$ and 200 GeV, respectively. The STAR detector consists of a 4.2 m long cylindrical time projection chamber (TPC) of 2 m radius. In 2000(2001) the TPC was operated in a 0.25(0.5) T solenoidal magnetic field. Particles are identified by their energy loss in the TPC. A central trigger barrel (CTB) of 240 scintillators surrounds the TPC. Two zero degree calorimeters (ZDC) at ± 18 m from the interaction point are sensitive to the neutral remnants of nuclear break-up.

Exclusive ρ^0 production in UPC has a distinctive experimental signature: the $\pi^+\pi^-$ decay products of the ρ^0 meson are observed in an otherwise 'empty' spectrometer. The tracks are approximately back-to-back in the transverse plane due to the small p_T of the pair. Two different triggers are used for this analysis. For $AuAu \rightarrow AuAu\rho^0$, about 30,000 (2000) and 1.5 M(2001) events were collected using a low-multiplicity 'topology' trigger. The CTB was divided in four azimuthal quadrants. Single hits were required in the opposite side quadrants; the top and bottom quadrants acted as vetoes to suppress cosmic rays. A fast on-line reconstruction removed events without reconstructible tracks from the data stream. To study $AuAu \rightarrow Au^*Au^*\rho^0$, about 0.8 M(2000) and 2.5 M(2001) 'minimum bias' events, which required coincident detection of neutrons from nuclear break-up in both ZDCs as a trigger, are used for the analysis.

Events are selected with exactly two oppositely charged tracks forming a common vertex within the interaction region. The specific energy loss dE/dx in the TPC shows that the event sample is dominated by pion pairs. In the topology triggered data sets, without the ZDC requirement, cosmic rays are a major background. They are removed by requiring that the two pion tracks have an opening angle of less than 3 radians. Figure 2 shows kinematic distributions for the selected 2-track events in the $\sqrt{s_{NN}} = 200$ GeV minimum bias data; these distributions are similar for the other data sets.

Figure 2a) shows the transverse momentum spectrum of oppositely charged pion-pairs (points). A clear peak, the signature for coherent coupling, can be observed at $p_T < 150$ MeV. Those events are compatible with coherently produced ρ^0 candidates. A background model from like-sign combination pairs (shaded histogram), which is normalized to the signal at $p_T > 250$ MeV, does not show such a peak. The open histogram is a Monte Carlo simulation [4] for coherent ρ^0 production accompanied by nuclear break-up superimposed onto the background. The dN^ρ/dp_T (i.e. the $dN^\rho/dt \sim dN^\rho/dp_T^2$) spectrum reflects not only the nuclear form factor, but also the photon p_T distribution and

the interference of production amplitudes from both gold nuclei. The interference arises since both nuclei can be either the photon source or the scattering target [6]. A detailed analysis of the $p_T(t)$ distribution is in progress.

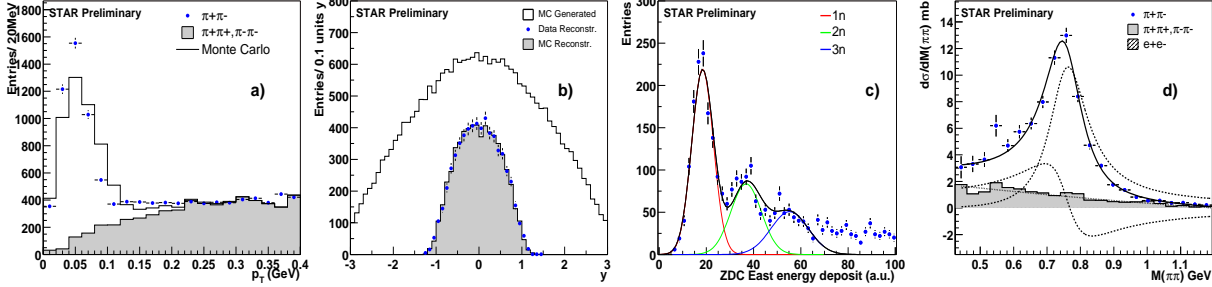


Figure 2. The (a) ρ^0 transverse momentum and (b) rapidity distribution, the (c) ZDC response, and (d) the $d\sigma/dM_{\pi\pi}$ invariant mass distribution for 2-track (xn,xn) events in the $\sqrt{s_{NN}}=200$ GeV minimum bias data.

The rapidity distribution in Fig. 2b) is well described by the reconstructed events from the Monte Carlo simulation. The generated rapidity distribution is also shown. The acceptance for exclusive ρ^0 is about 40% at $|y_\rho| < 1$. At $|y_\rho| > 1$, the acceptance is small and this region is excluded from the analysis; the cross sections are extrapolated to the full 4π acceptance with the Monte Carlo simulation. Using the energy deposits in the ZDCs (Fig. 2c)), we select events with at least one neutron (xn,xn), exactly one neutron (1n,1n), or no neutrons (0n,0n) in each ZDC; the latter occurs only in the topology trigger.

Figure 2d) shows the $d\sigma/dM_{\pi\pi}$ spectrum for events with pair- $p_T < 150$ MeV/c (points). The fit (solid) is the sum of a relativistic Breit-Wigner for ρ^0 production and a Söding interference term for direct $\pi^+\pi^-$ production [7] (both dashed). A second order polynomial (dash-dotted) describes the combinatorial background (shaded histogram) from grazing nuclear collisions and incoherent photon-nucleon interactions. Incoherent ρ^0 production, where a photon interacts with a single nucleon, yields high p_T ρ^0 s, which are suppressed by the low pair p_T requirement; the remaining small contribution is indistinguishable from the coherent process. A coherently produced background arises from the two-photon process $AuAu \rightarrow Au^{(*)}Au^{(*)}l^+l^-$. It contributes mainly at low invariant mass $M_{\pi\pi} < 0.5$ GeV/c². The small contribution from ω decays is neglected.

Figure 3 compares our results on cross sections for coherent ρ^0 production at $\sqrt{s_{NN}} = 130$ GeV[8] to the calculations of Ref. [4]. Preliminary results for $\sqrt{s_{NN}} = 200$ GeV are also shown in the plot. The cross sections are obtained from the integral of the Breit-Wigner fit, extrapolated to full rapidity. The integrated luminosity for the minimum bias data is determined from the number of hadronic interactions, assuming a total gold-gold hadronic cross section of 7.2 b [5]. For coherent ρ^0 production accompanied by mutual nuclear break-up (xn,xn), we measure a cross section of $\sigma(AuAu \rightarrow Au_{xn}^*Au_{xn}^*\rho^0) = 39.7 \pm 2.8 \pm 9.7$ mb. By

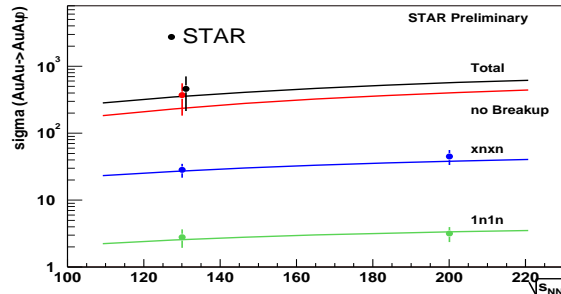


Figure 3: Comparison to predictions from Ref. [4].

Figure 3 compares our results on cross sections for coherent ρ^0 production at $\sqrt{s_{NN}} = 130$ GeV[8] to the calculations of Ref. [4]. Preliminary results for $\sqrt{s_{NN}} = 200$ GeV are also shown in the plot. The cross sections are obtained from the integral of the Breit-Wigner fit, extrapolated to full rapidity. The integrated luminosity for the minimum bias data is determined from the number of hadronic interactions, assuming a total gold-gold hadronic cross section of 7.2 b [5]. For coherent ρ^0 production accompanied by mutual nuclear break-up (xn,xn), we measure a cross section of $\sigma(AuAu \rightarrow Au_{xn}^*Au_{xn}^*\rho^0) = 39.7 \pm 2.8 \pm 9.7$ mb. By

selecting single neutron signals in both ZDCs, we obtain $\sigma(AuAu \rightarrow Au_{1n}^* Au_{1n}^* \rho^0) = 2.8 \pm 0.5 \pm 0.7$ mb. The systematic uncertainties are dominated by the uncertainties of the luminosity determination and the 4π extrapolation. The absolute efficiency of the topology trigger is poorly known and does not allow a direct cross section measurement. From $\sigma(AuAu \rightarrow Au_{xn}^* Au_{xn}^* \rho^0)$ and the ratio $\sigma_{xn,xn}^\rho / \sigma_{0n,0n}^\rho$ we estimate $\sigma(AuAu \rightarrow AuAu\rho^0) = 370 \pm 170 \pm 80$ mb and the total cross section for coherent ρ^0 production $\sigma(AuAu \rightarrow Au^{(*)} Au^{(*)} \rho^0) = 460 \pm 220 \pm 110$ mb.

Two-photon interactions include the purely electromagnetic process of e^+e^- pair production as well as single and multiple meson production. The coupling $Z\alpha$ (0.6 for Au) is large, so e^+e^- pair production is an important probe of quantum electrodynamics in strong fields [1]. At momenta below 125 MeV, e^+e^- pairs are identified by their energy loss in the TPC as shown in Fig. 4a) for a $\sqrt{s_{NN}} = 200$ GeV minimum bias data sample. This data was taken with a 0.25 T magnetic field; at the full 0.5 T field the low momentum electrons are bent out of the acceptance.

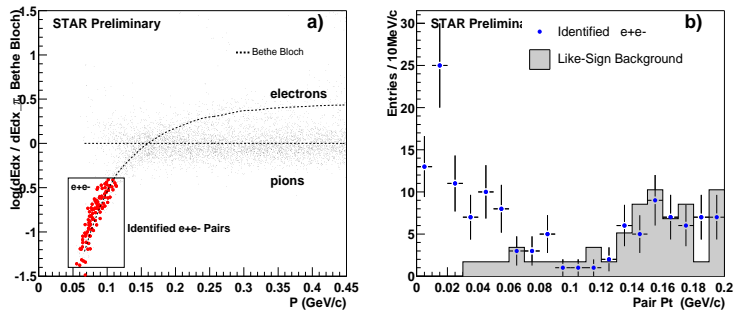


Figure 4: (a) Energy loss dE/dx of tracks in the 2-track, $\sqrt{s_{NN}} = 200$ GeV minimum bias data with reduced magnetic field. The dots indicate events where both particles are identified as electrons. (b) The p_T spectrum for identified e^+e^- pairs.

Figure 4b shows the p_T spectrum for identified e^+e^- pairs; a clear peak at $p_T \sim 1/b < 20$ MeV/c identifies the process $AuAu \rightarrow Au^*Au^*e^+e^-$.

In summary, ultra-peripheral heavy-ion collisions are a new laboratory for diffractive interactions, complementary to fixed-target ρ^0 photo-production on complex nuclei [9]. The first measurements of coherent ρ^0 production with and without accompanying nuclear excitation, $AuAu \rightarrow Au^*Au^*\rho^0$ and $AuAu \rightarrow AuAu\rho^0$, confirm the existence of vector meson production in ultra-peripheral heavy ion collisions. The cross sections at $\sqrt{s_{NN}} = 130$ and 200 GeV are in agreement with theoretical calculations.

REFERENCES

1. G. Baur *et al.*, Phys. Rept. **364**, 359 (2002).
2. C. F. v. Weizsäcker, Z. Phys. **88**, 612 (1934); E.J. Williams, Phys. Rev. **45**, 729 (1934).
3. J.J. Sakurai, Ann.Phys.**11** 1 (1960); T.H. Bauer *et al.*, Rev.Mod.Phys.**50** 261 (1978).
4. S. R. Klein and J. Nystrand, Phys. Rev. C **60**, 014903 (1999); J. Nystrand, A. J. Baltz and S. R. Klein, Phys. Rev. Lett. **89** 012301 (2002).
5. A. J. Baltz, C. Chasman, and S. N. White, Nucl. Instrum. Methods **A417**, 1 (1998).
6. S. R. Klein and J. Nystrand, Phys. Rev. Lett. **84**, 2330 (2000).
7. P. Söding, Phys. Lett. **19**, 702 (1966);
8. C. Adler *et al.*, submitted to Phys. Rev. Lett., nucl-ex/0206004.
9. F. Bulos *et al.*, Phys. Rev. Lett. **10**, 490 (1969); H. Alvensleben *et al.*, Phys. Rev. Lett. **24**, 786 and 792 (1970), and Nucl. Phys. B18, 333 (1970); G. McClellan *et al.*, Phys. Rev. **D4**, 2683 (1971).